Tellus (1985), *37A*, 106–125

The thermally coupled response of the planetary scale circulation to the global distribution of heat sources and sinks

By DONALD R. JOHNSON, *Department of Meteorology, Space Science and Engineering Center, University of Wisconsin-Madison, 1225 West Dayton Street, Madison, Wisconsin 53706, USA*, RONALD D. TOWNSEND*, *Department of Meteorology, University of Wisconsin-Madison* and MING-YING WEI, *Space Science and Engineering Center, University of Wisconsin-Madison*

(Manuscript received June 27, 1983; in final form July 3, 1984)

ABSTRACT

The time-averaged structure of global monsoonal circulations and planetary scale transport processes are determined from the FGGE Level IIIa operational data set generated by the US National Meteorological Center. Through isentropic diagnostics, rotational and irrotational components of the horizontal mass transport and the distribution of heating for the planetary scale are analyzed for the months of January, April, July and October of 1979. The global monsoonal circulations coupled with the planetary scale of differential heating occur in the form of large scale Hadley-type and Walker-type circulations. Net heating within a given region and net cooling in another region in association with latent heat release and differences in boundary flux of energy through the earth's surface and the top of the atmosphere result in forcing of isentropic mass circulations that link energy source with energy sink regions, a result basic to thermally forced circulations. The primary planetary source of energy in the region of Indonesia–Philippines–Southeast Asia is linked through isentropic mass transport with sinks of energy in the regions of the two circumpolar vortices, the Sahara and subtropical anticyclonic circulations. This primary center of the source of energy in the Indonesia–Southeast Asia area moves seasonally from one hemisphere to the other. Other source regions of energy occur over Brazil in January and Central America and Africa in July.

Through horizontal transport of mass and energy, the winter Asiatic monsoonal circulation links radiative cooling over Asia to sensible and latent heat release within mid-latitude baroclinic waves and also to latent heat release in the Indonesia, Philippine and New Guinea regions. The rôle of mid-latitude baroclinic waves in providing for mass and energy exchange between polar and subtropical regions within the time-averaged isentropic structure is briefly discussed.

1. Introduction

Forty years ago, Sir Napier Shaw (1942) discussed the planetary scale of mass exchange within an isentropic structure of the atmosphere and pointed towards the concept of thermally forced planetary scale circulations. After dividing the atmosphere into an overworld of warmer air spanning the entire meridional extent of the atmosphere and an underworld of colder air restricted to higher latitudes, he emphasized that the overworld exchanged properties with the underworld through convection associated with diabatic processes. No exchange would be realized with adiabatic motion through which the geometric forms of the isentropic surfaces evolved. In the isentropic analysis of the planetary scale mass and energy transport from a FGGE (First GARP Global Experiment) data set presented herein, results that isolate a thermally

* Present Affiliation: Air Command and Staff College, Maxwell AFB, AL 36112, USA.

coupled component of planetary scale circulations and the diabatic convective exchange through isentropic surfaces suggested by Sir Napier Shaw are now discussed.

Within a transient atmosphere, the thermally coupled component of mass circulation may be small compared to exchange by other dynamical processes. However, for the time-averaged circulation, the combination of stratification and diabatic heating permit inference between the horizontal scales of differential heating and of mass and energy transport. For a quasi-steady time-averaged mass distribution, the irrotational component of the mass circulation is uniquely related to differential heating. Within the heat source region, the mass transport is convergent in lower isentropic layers and divergent in upper layers. Within the heat sink region, the mass transport is divergent in lower layers and convergent in upper layers. Thus, a thermally coupled component of horizontal mass transport from a heat source to a heat sink must occur in upper isentropic layers while a component of the mass transport must be from heat sink to heat source in lower layers. Such transport is necessary to satisfy the continuity requirement that mass transport is upward relative to isentropic surfaces in the heat source region and downward in the heat sink region.

The link between mass and energy transport is also interesting. Regions of heating are energy sources, while regions of cooling are energy sinks. Within the isentropically time-averaged atmosphere, the vertical energy flux is upward in regions of heating and the quasi-horizontal energy flux is divergent in upper layers and convergent in lower layers. In regions of cooling, the vertical energy flux is downward with horizontal flux being convergent in upper layers and divergent in lower layers. Thus, the scales of mass and energy transport from heat source to the heat sink in higher isentropic layers and from heat sink to heat source in lower isentropic layers are equivalent. With respect to the vertically integrated flow, the divergence of the time-averaged mass transport must vanish while the net transport of energy is from the heat source to the heat sink.

The purpose of this paper is to provide a descriptive analysis of the planetary scale isentropic mass circulation and corresponding diabatic heating determined from the National Meteorological Center (NMC) FGGE Level IIIa data set. Insight into seasonal variation is provided from comparing analyses for the months of January, April, July and October, 1979. Particular emphasis is placed on isolating the thermally coupled component of the isentropic mass transport and showing its relation to the global distribution of differential heating. The discussion will also point to a link that must exist between thermally coupled components of the mass and energy transport (Johnson et al., 1981).

2. Quasi-horizontal mass transport

The quasi-horizontal mass transport embedded within an isentropic layer is represented by time-averaged mass transport potential ($\bar{\chi}$) and stream ($\bar{\psi}$) functions through the use of Helmholtz's theorem given by

$$\overline{\rho J \boldsymbol{U}} = \nabla_\theta \bar{\chi} + \boldsymbol{k} \times \nabla_\theta \bar{\psi}, \tag{1}$$

where the irrotational and rotational components of the mass transport are defined by

$$(\rho J \boldsymbol{U})_\chi = \nabla_\theta \chi \tag{2}$$

$$(\rho J \boldsymbol{U})_\psi = \boldsymbol{k} \times \nabla_\theta \psi. \tag{3}$$

(See Appendix for list of symbols. Where no ambiguity exists, the superscript t of the temporal averaging operator $(\bar{\ })^t$ is suppressed.) The Poisson equations used to determine $\bar{\chi}$ and $\bar{\psi}$ through vector operations in (1) are

$$\nabla_\theta^2 \bar{\chi} = \nabla_\theta \cdot (\overline{\rho J \boldsymbol{U}}) = \delta, \tag{4}$$

$$\nabla_\theta^2 \bar{\psi} = \boldsymbol{k} \cdot \nabla_\theta \times (\overline{\rho J \boldsymbol{U}}) = \zeta. \tag{5}$$

With the divergence and curl of the mass transport estimated from NMC's global FGGE Level IIIa analyses, numerical solutions from a centered finite difference analogue of the Poisson equations (4) and (5) were computed on a five-degree latitude–longitude grid by the method of successive over-relaxation (Young, 1962). The functions are uniquely determined with the exception of a constant of integration since no lateral boundary conditions exist for the global domain. In regions where an isentropic layer intersects the earth's surface, the use of the Lorenz convention (Dutton and Johnson, 1967) to define isentropic surfaces beneath the earth's surface permits retention of a global domain for the relaxation. Within a "hydro-

static" isentropic layer which lies beneath the earth's surface, ρJ (equal $g^{-1}|\partial p/\partial\theta|$) is zero from the Lorenz convention that $p(\lambda,\phi,\theta,t) = p(\lambda,\phi,\theta_s,t)$ for $\theta \leqslant \theta_s$. This convention implies that "underground" isentropic surfaces are contiguous with the earth's surface. When the lower surface of an isentropic layer intersects the earth's surface, the mass ρJ is specified by $p(\lambda,\phi,\theta,t) - p(\lambda,\phi,\theta_s,t)$. Zillman (1972) presents details on the numerical methods and tests of convergence in using this method to calculate the mass transport potential from climatological analysis of diabatic heating for the Southern Hemisphere.

3. Mass balance of the time-averaged state

The time-averaged equation of mass continuity expressed in isentropic coordinates is

$$\frac{\partial}{\partial t_\theta}\overline{(\rho J)} + \nabla_\theta \cdot \overline{(\rho J \boldsymbol{U})} + \frac{\partial}{\partial\theta}\overline{(\rho J\dot{\theta})} = 0. \tag{6}$$

With the time-average over a sufficiently long interval to invoke the quasi-steady assumption and use of (4), the balance between the horizontal divergence of the mass transport and the vertical derivative of the diabatic mass flux is given by

$$\nabla_\theta \cdot \overline{(\rho J \boldsymbol{U})} = \nabla_\theta^2 \bar{\chi} = -\frac{\partial}{\partial\theta}\overline{(\rho J\dot{\theta})}. \tag{7}$$

Horizontal mass convergence (divergence) is balanced by an increase (decrease) of the upward mass flux relative to isentropic surfaces in regions of heating or a decrease (increase) of the downward mass flux relative to isentropic surfaces in regions of cooling. The mass potential function will tend to be a relative maximum (minimum) in regions of convergence (divergence).

With a vertical integration and the assumption that the vertical mass transport vanishes at the top of the atmosphere θ_T, the vertical mass flux through an isentropic surface is

$$\overline{\rho J\dot{\theta}} = \int_\theta^{\theta_1} \nabla_\theta \cdot \overline{(\rho J \boldsymbol{U})}\,\mathrm{d}\theta \tag{8}$$

$$= \int_\theta^{\theta_1} \nabla_\theta^2 \bar{\chi}\,\mathrm{d}\theta. \tag{9}$$

This form of the continuity equation shows the unique relation between the diabatic mass flux at an isentropic level and the net mass divergence within the overlying atmosphere. The diabatic heating rate defined as the mass-weighted average of the vertical mass flux is given by

$$\bar{\dot{\theta}} = \overline{\rho J\dot{\theta}}/\overline{\rho J}. \tag{10}$$

The corresponding temporally and vertically averaged quantity is

$$\bar{\dot{\theta}}^{\theta,t} = \overline{\rho J\dot{\theta}}^{\theta,t}/\overline{\rho J}^{\theta,t}. \tag{11}$$

In estimating the vertical mass flux, the constraint that the vertically integrated mass divergence vanishes is imposed. This constraint stems from the steady state assumption and the use of the Lorenz convention within the time-averaged state. The lowest surface of the isentropic domain is determined by the coldest potential temperature, θ_{s_0}, that is observed at the earth's surface during the time averaging interval. Within the "underground" portion of the isentropic domain, i.e., θ_{s_0} to $\theta(\lambda,\phi,z_s,t)$, the mass ρJ is zero. Thus the vertical mass flux vanishes on all "underground" isentropic surfaces. This constraint in conjunction with the upper boundary condition requires that the vertically integrated divergence of the horizontal mass transport vanish. The balance between the mass transport and the heating distribution is thermodynamic in the sense that it does not explicitly involve momentum exchange. The balance of forces that maintain the rotational and irrotational components of the isentropic mass transport would be determined through an analysis of the tendencies of $\nabla_\theta \cdot (\rho J \boldsymbol{U})$ and $\boldsymbol{k} \cdot (\nabla_\theta \times \rho J \boldsymbol{U})$. The present discussion emphasizes that a thermodynamic component of the mass transport can be isolated which is directly linked with heating.

4. The mass balance of planetary scale circulation inferred from FGGE Level IIIa data

The results for mass transport presented in this study were determined from the FGGE Level IIIa data set generated by the NMC global data assimilation system. The characteristics of this data set and NMC's optimum interpolation data assimilation system were described by NMC's Staff Atmospheric Analysis Branch (1979); Fleming et al. (1979a); Fleming et al. (1979b); Bergman (1979); and McPherson et al. (1979).

The isobaric data set consists of twice daily global analysis fields for 12 selected levels from 1000 to 50 mb on a 2.5° latitude–longitude grid. The period of the data set is from December 1978 through November 1979. The meteorological variables include zonal and meridional wind components, temperature, geopotential height and surface pressure.

An isentropic data set of pressure, zonal and meridional wind components and Montgomery stream function were produced from the same grid and observation times at 16 isentropic levels with a 10 K vertical resolution by linear interpolation with θ^1/κ. The vertical extent of the isentropic fields varies from Northern to Southern Hemispheres and from month to month since the data is processed by hemispheres and the 16 levels depend explicitly on the minimum surface potential temperature. For any given observation time, the vertical extent always reaches 370 K. This includes nearly all of the planetary tropospheric circulation.

The pattern of large scale transport processes was evident from calculations using either a 5° or 2.5° grid resolution. In view of the focus on the planetary scale circulation and economical considerations, the mass transport potential and stream functions were generated on the 5° grid. Elimination of smaller scale details evident in the 2.5° grid did not affect the pattern of the large scale transport processes.

Analysis of the quasi-steady assumption verified that the local time rate of change of mass was at least one order of magnitude smaller than the horizontal divergence of mass transport for the time span of a month. The requirement that the vertically integrated mass divergence vanish was imposed by using a mass weighted adjustment where the original non-zero value is distributed vertically according to the amount of mass contained in the isentropic layers (Wei et al., 1983). For the periods considered, the average adjustment is generally within 20% of the maximum mass divergence of the original profile and the regional distribution of divergence and convergence is essentially unchanged.

For the computation of diabatic heating, two filtering techniques are applied to fields of quasi-horizontal mass divergence. Zonal harmonics with wavelengths less than 4000 km are first deleted through truncation of one-dimensional Fourier transforms. See Wei et al. (1983) for a table of typical % variances retained in the mass divergence. Spatial smoothing is then accomplished by applying a low pass filter and an inverse filter in both east–west and north–south directions (Holloway, 1958). The low pass filter has weights (1,2,1) and the inverse filter (−1,5,−1). The response of this combination is roughly 50% for a wavelength of 5 grid increments. The large scale patterns of heating and cooling determined with filtering were essentially unaltered from patterns determined without filtering. Monthly averaged mass transport potential and stream functions and vertically averaged diabatic heating, are now presented for January, April, July and October 1979.

4.1. The mean global transport of mass for January 1979

Irrotational and rotational components of the isentropic mass transport portrayed through potential and stream functions will be presented for selected levels that capture the nature of the planetary scale monsoonal circulations. The global scale circulations are described well by the 300–310 K and 340–350 K isentropic layers. At higher latitudes of the Northern Hemisphere, a mass circulation exists within lower layers that couples the wintertime exchange of polar air masses between continental and oceanic regions. This exchange which primarily occurs below 300 K is an important feature of the winter monsoon. Its pattern will be delineated by irrotational component of mass transport for the 260–270 K, 270–280 K, 280–290 K, and 290–300 K isentropic layers. More emphasis will be given to the irrotational component in view of its direct link with the time-averaged planetary scale differential heating. While this component is small in magnitude relative to the rotational component particularly in mid and higher latitudes, its importance is not. Viewed simply, this component is fundamental to all monsoonal circulations.

The mass transport stream and potential functions for the 300–310 K and 340–350 K isentropic layers for January are displayed on Mercator map projections in Fig. 1. Since the transport processes are proportional to the gradient of these fields and the constant of integration is arbitrary, no physical relevance should be attached to a particular isopleth in a comparison of the fields displayed in the different figures.

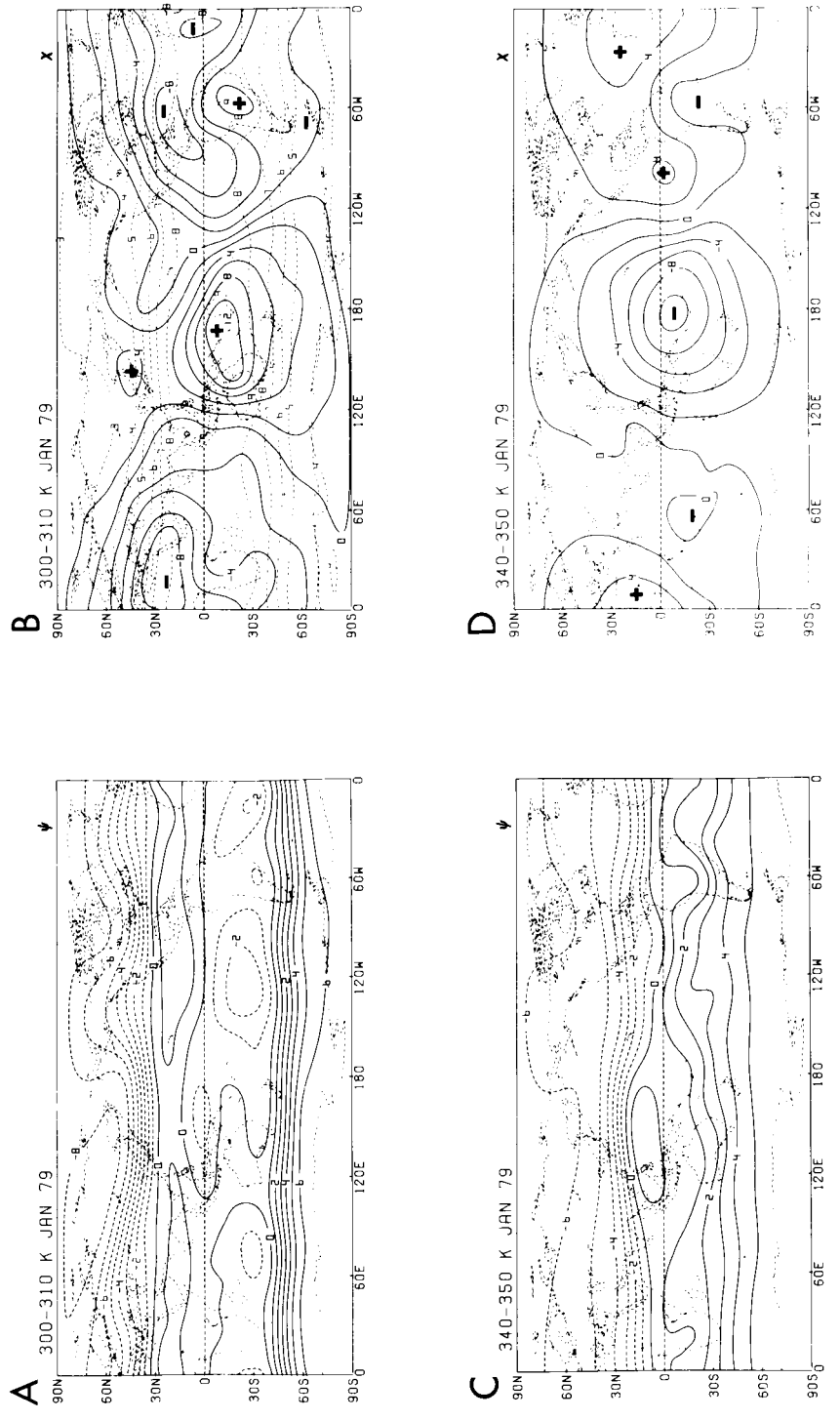

Fig. 1. Mass stream (ψ) and transport potential (χ) functions for the 300–310 K (a and b) and 340–350 K (c and d) isentropic layers of January 1979 (units, a and c 10^9 kg K^{-1} s^{-1}; b and d 10^8 kg K^{-1} s^{-1}). Rotational component of isentropic mass transport, ρU_ϕ, is parallel to the contours of $\bar{\psi}$ with lower values to the left. Irrotational component of isentropic mass transport, ρU_λ, is perpendicular to the contours of $\bar{\chi}$ from lower to higher values. Plus and minus signs in the potential field indicate relative maxima and minima, respectively. Dashed contours in (b) and (d) represent the mean pressure of the isentropic (units, 10^2 mb).

The mean pressure topography of each isentropic layer is indicated by the dashed lines in the panels of mass transport potential. The sloping nature of the 300–310 K layer from the low tropical troposphere to the high polar troposphere is evident in Fig. 1b. In the tropical regions, the 300–310 K layer is located near 800 mb over oceanic regions and near 900 mb over the warmer continental regions of South America and Australia. At northern polar latitudes, this layer ascends to 300 mb; over the Antarctic continent, the layer is located above 400 mb. The maximum slope of the 300–310 K layer occurs within the westerly wind regimes of both hemispheres (Figs. 1a and b). From the pressure topography, it is evident that quasi-horizontal transport of mass within this layer couples the low troposphere of the tropical and subtropical regions with the high troposphere of polar latitudes.

The pressure analysis for the 340–350 K layer in Fig. 1d reveals little horizontal variation. For the Southern Hemisphere, the 340–350 K layer lies between the 300 and 200 mb levels while in the Northern Hemisphere the surface lies near 200 mb. Thus, the 340–350 K layer is relatively horizontal and lies within the high tropical–subtropical troposphere and low polar stratosphere. Mass circulations within this layer link these two portions of the atmosphere and provide evidence of stratospheric/tropospheric exchange of mass and other atmospheric properties (Johnson, 1979).

Several interesting features of the westerly circulations in both hemispheres are evident in the mass stream function of the 300–310 K isentropic layer (Fig. 1a). The rotational components of the momentum in the Northern and Southern Hemispheres are most intense in middle and higher latitudes. The larger amplitude wave structure of the Northern Hemisphere flow, in contrast with the more zonal flow of the Southern Hemisphere, reflects the influence of continents and oceans in the Northern Hemisphere. The ridging over Alaska, the Gulf of Alaska and western United States and the deep trough over the eastern half of the United States are features of the severe winter circulation of 1978–79 over North America. The intense westerlies inferred from the stream function over the eastern portions of the United States is associated with the strong temperature contrast between the extremely cold polar air during this season that lies in close proximity with the warmer subtropical air. Over the Asiatic mainland and the western Pacific, the intense stream function gradient is again evidence of the strong westerlies normally occurring during the winter season in this region. In this case, the flow appears to be more zonal during January 1979 and likely reflects lesser meridional exchange than in the North American region. Subtropical anticyclonic circulations in the Southern Hemisphere are evident over the Atlantic, Pacific and Indian Ocean regions. The subtropical anticyclonic circulations in the Northern Hemisphere in the 300–310 K isentropic layer are not as distinct during the winter season.

Many mid-latitude features in the mass stream function of the 300–310 K isentropic layer are similar to features found in isobaric analyses of the 500 mb flow. Note in Fig. 1b that the mean pressure of the 300–310 K layer in extratropical latitudes is near the mid troposphere. In lower latitudes the pattern of the mass stream function is more similar to an 850 mb pattern since the 300–310 K layer in these regions is located in the lower troposphere.

The analyses for the mass stream function within the 340–350 K layer (Fig. 1c) show strong westerlies in subtropical latitudes of the Northern Hemisphere and a weaker westerly regime extending from tropical latitudes to mid-latitudes in the Southern Hemisphere. A poleward displacement of the strong gradient of the stream function of the 300–310 K layer (Fig. 1a) with respect to that in the 340–350 K layer (Fig. 1c) is evident. This displacement points out that the rotational component of the subtropical jet stream occurs at lower latitudes within the 340–350 K layer while the same component of the polar jet stream is distinctly displaced towards higher latitudes in the 300–310 K layer.

The latitudinal and layered separation of the polar jet stream from its subtropical counterpart within isentropic coordinates is identified in part with the gradient of the mass distribution that occurs across jet streams. The Laplacian of the isentropic mass stream function is composed of two terms,

$$\nabla_\theta^2 \bar{\psi} = \boldsymbol{k} \cdot |\overline{\nabla_\theta \times (\rho J \boldsymbol{U}|} = \overline{\rho J \boldsymbol{k} \cdot (\nabla_\theta \times \boldsymbol{U})} + \overline{\boldsymbol{k} \cdot (\nabla_\theta \rho J \times \boldsymbol{U})}. \quad (12)$$

One is determined from the product of the mass distribution and the vertical component of the

vorticity field and the other by the vertical component of the cross product of the gradient of mass and velocity. Within equivalent barotropic regions of the westerlies, the last term is simply the product of the magnitudes of $\nabla_\theta \rho J$ and $\boldsymbol{U}$. This term is large within hyperbaroclinic zones of mid-latitudes that are located beneath and within the jet stream and the tropopause break. The corresponding definition for the isobaric mass stream function only consists of the first term and is determined solely by the vorticity distribution. The latitudinal displacement of the strong gradient of the stream function towards low latitudes in the 340–350 K layer is a reflection of the gradient of mass within the tropopause break of the subtropical jet stream.

Differences in the latitudinal domains of the westerlies within the two layers are also expected from the two distinct direct cells embedded within the isentropic zonally averaged Hadley circulation that spans the Northern Hemisphere. See Fig. 2 (from Townsend and Johnson, 1981). The upper tropospheric westerlies are maintained by poleward transport of angular momentum. The pattern of the rotational component of the mass transport in the 340–350 K layer indicates that the embedded ageostrophic Hadley circulation of low latitudes is linked with the maintenance of the subtropical jet (Krishnamurti, 1961). The maintenance of a polar jet as an entity separate from the subtropical jet is related to the embedded direct geostrophic meridional cell in mid-latitudes. This mid-latitude cell occurs in conjunction with sources of latent and sensible heat associated with baroclinic waves and extratropical cyclones.

The mass transport potential functions for the 300–310 K and 340–350 K layers (Figs. 1b and d) portray the component of mass transport that links heat sources with heat sinks. Fig. 3 shows the planetary scale distribution of the vertically averaged diabatic heating for the four months selected in this study. A similarity of horizontal

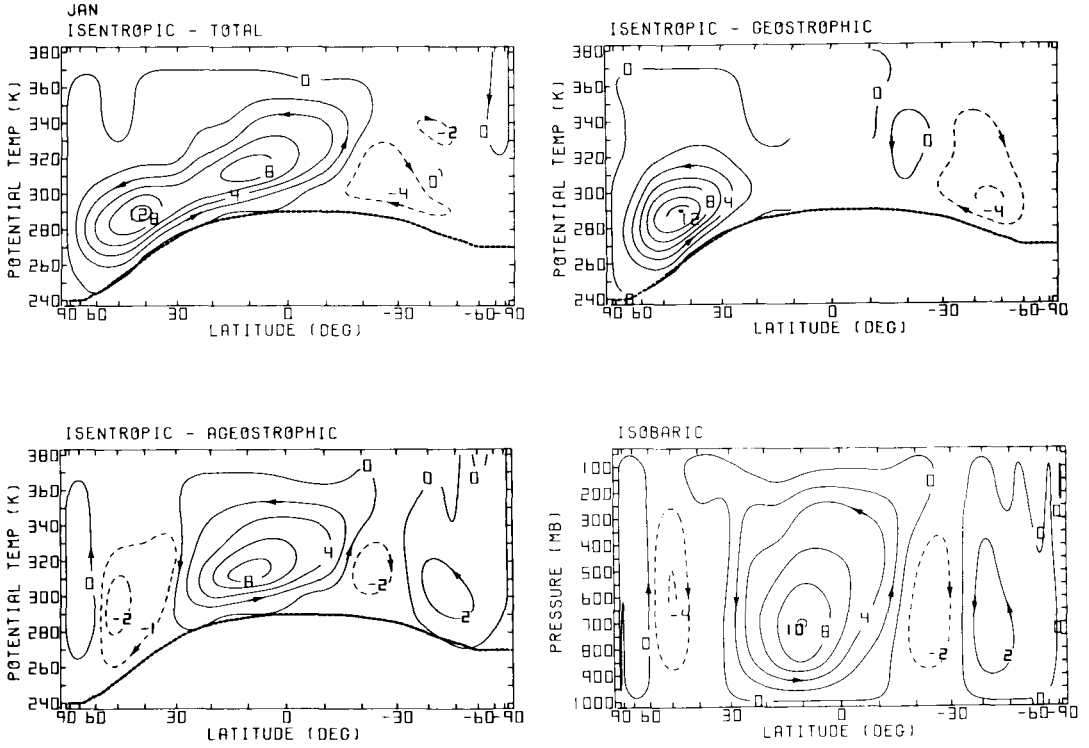

Fig. 2. Mass stream function for isentropic and isobaric zonally averaged meridional circulations for January 1979 (units, 10^{10} kg s^{-1}). Arrows indicate the direction of the circulation (from Townsend and Johnson, 1981).

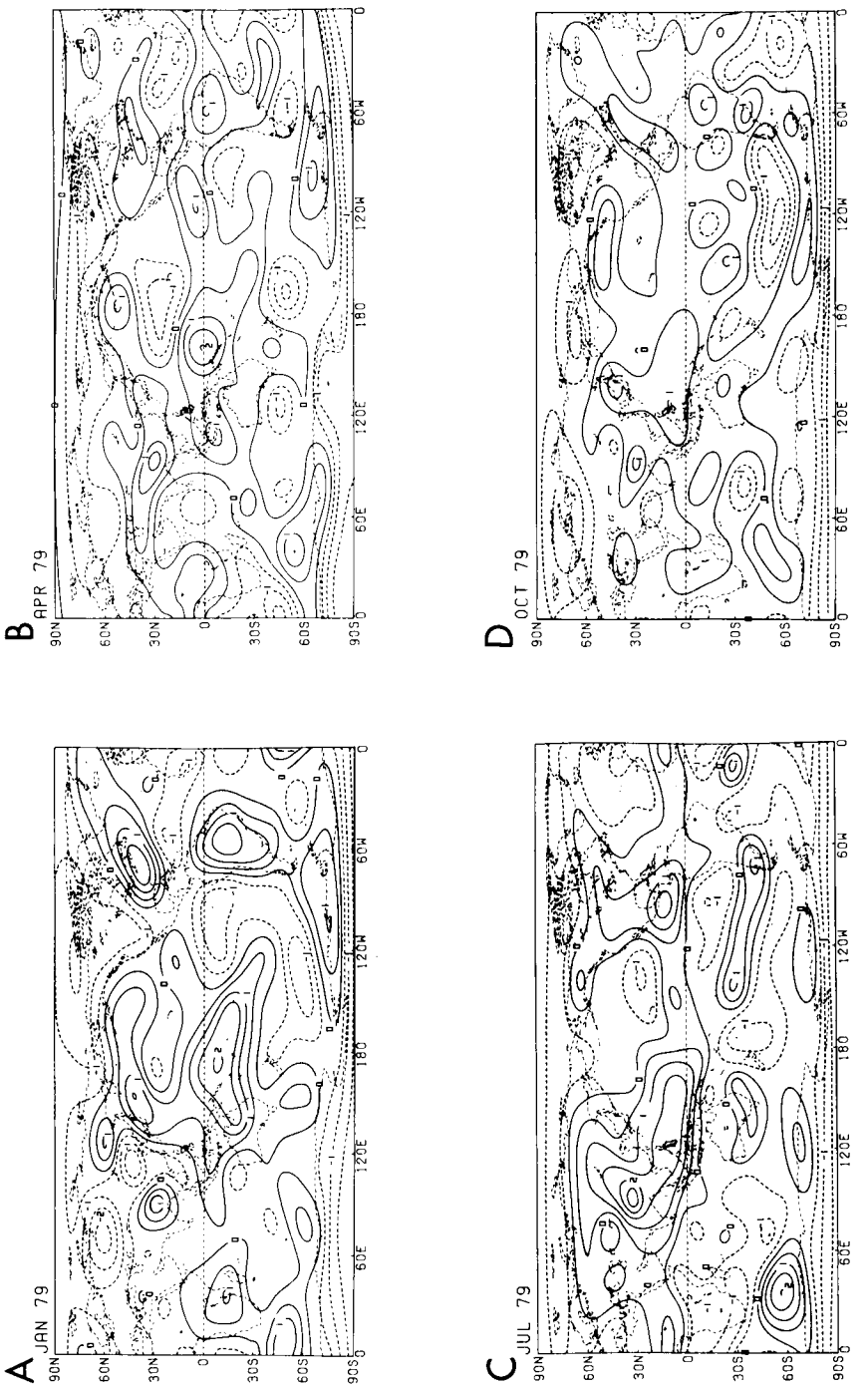

Fig. 3. Mass weighted vertically averaged diabatic heating rates (K day^{-1}) for January (a), April (b), July (c) and October (d) 1979.

scales is evident from comparison of the two distributions. From the continuity constraint expressed by (8) and (9), the patterns of the potential functions for the layers in Fig. 1 being inverse to each other indicate the two-layered nature of the response of the planetary scale mass transport to differential heating. The strong meridional and zonal gradients of the transport potential are evidence of both Hadley-type and Walker-type circulations that span the entire globe.

In January, a primary heat source of the planetary circulation is located in the western tropical Pacific to the northeast of Australia (Fig. 3a); the mass transport is convergent within the 300–310 K layer and divergent in the 340–350 K layer (Figs. 1b and d). The quasi-circular nature of the 340–350 K potential function that spans radially 6000 to 7000 km indicates equal importance of the zonal and meridional components of the thermodynamically coupled mass transport. This mass divergence in the 340–350 K layer over the western tropical Pacific is linked with convergence over regions of cooling in the polar latitudes, Sahara, the adjacent eastern Atlantic region and eastern equatorial Pacific. Johnson et al. (1981) have shown that energy transport may be inferred from the mass circulation. These results show that the irrotational mode of mass transport links regions of energy excess and deficit by diabatic processes. The energy balance of the subtropical anticyclones and desert regions in the tropics is maintained through subsidence in association with the mass convergence in the high troposphere, the primary source of energy being through horizontal transport from the regions of convection in the western tropical Pacific.

Within the 300–310 K layer (Fig. 1b), note the relatively strong equatorward irrotational component of the mass transport from the Southern Hemisphere circumpolar vortex and the western subtropical north Pacific into the region of convection in the western equatorial Pacific. This pattern indicates strong tropical–extratropical coupling in both the Southern and Northern Hemispheres. The divergent mode of mass transport just east of the Philippines is part of the Asiatic winter monsoonal flow within the low troposphere through which the atmosphere acquires sensible and latent energies in its equatorward motion. Note the diabatic heating in the region of the Asiatic winter monsoonal flow just east of the China coast. The mass and energy transport from the higher latitudes is in effect a source of heat through horizontal convergence within the low tropical troposphere that helps to maintain a vertical structure favorable for the deep convection in those regions. Concepts of atmospheric circulation based on ideas that the maintenance of convection within the tropics occurs through "in situ" sources of latent and sensible energies are oversimplified.

Another noteworthy feature in Fig. 1b is the smaller scale regions of mass convergence over South America and over Africa in the vicinity of Madagascar. Both are regions of intense convection and source regions of energy in addition to the tropical region of the western Pacific (Fig. 3a).

The global scale isentropic mass circulations described above are in general agreement with those inferred from the climatological distribution of heating for the Northern Hemisphere by Otto-Bliesner and Johnson (1982) and for the Southern Hemisphere by Zillman and Johnson (1985). Within tropical latitudes, they also agree with results based on isobaric analyses from Flohn (1971), Krishnamurti (1971), Krishnamurti et al. (1973), and Murakami and Unninayar (1977), and Bengtsson et al. (1982).

The reasons for the similarity of isentropic and isobaric potential functions in tropical latitudes stem from a combination of the definition of mass transport and the nature of mass distribution. From the relation

$$\nabla_\theta^2 \bar{\chi} = \nabla_\theta \cdot \overline{(\rho J \boldsymbol{U})} = \overline{\rho J \nabla_\theta \cdot \boldsymbol{U}} + \overline{\boldsymbol{U} \cdot \nabla_\theta \rho J}, \tag{13}$$

the Laplacian of the potential function involves two terms, the one determined from the product of the mass and velocity divergence and the other from the advection of mass.

With the tropical atmosphere being largely barotropic, (13) is approximated by

$$\nabla_\theta^2 \bar{\chi} \simeq \rho J \overline{\nabla_\theta \cdot \boldsymbol{U}}. \tag{14}$$

Thus, isentropic and isobaric velocity divergence tend to equality. These simplifying conditions are expressed by

$$\nabla_\theta^2 \bar{\chi}_\theta / \overline{\rho J} \simeq \overline{\nabla_\theta \cdot \boldsymbol{U}} \simeq \overline{\nabla_p \cdot \boldsymbol{U}} = \nabla_p^2 \bar{\chi}_p, \tag{15}$$

where the subscripts θ and p indicate the isentropic and isobaric coordinates, respectively. Thus, in tropical regions the isentropic and isobaric potential functions are similar and the horizontal scales

of both, correspond with that of differential heating.

In mid-latitudes, mass divergence is no longer dominated by the first term of (13) and the isentropic mass circulation involves combinations of velocity divergence and mass advection. Within isobaric coordinates, the mass advection term and the mass weighting of velocity divergence vanish since mass within an isobaric layer is uniform. The contrast between the isobaric and isentropic zonally averaged circulations in Fig. 2 clearly shows these differences as well as the geostrophic and ageostrophic components of the isentropic mass circulation. Note the similarity between the ageostrophic isentropic circulation and the isobaric mass circulation which is restricted to ageostrophic motion. Note also the dominance of the geostrophic mass circulation in higher latitudes. Geostrophic mass advection is fundamental to isolating isentropic Hadley mass circulations of hemispheric extent since the process is a degree of freedom that directly relates the irrotational components of mass circulations of amplifying baroclinic waves to the net heating of the tropics and net cooling of higher latitudes (Johnson, 1979).

The irrotational components of the isentropic mass circulations presented for the Northern Hemisphere in Fig. 4 for the four lower isentropic layers ranging from 260–270 K to 290–300 K capture the exchange of polar air between continental and oceanic regions. Through this exchange, the ocean is in effect a mid-latitude source of energy to the atmosphere. The strong gradient of the mass transport potential over Japan, the northern Pacific, as well as Nova Scotia and the northern Atlantic shows the intensity of winter monsoonal flow with polar air moving equatorward and zonally from continental regions to the oceanic areas over the Gulf Stream and Kuroshio Current.

Within the 260–270 K and 270–280 K layers (Figs. 4a and b), the mass transport is divergent over Arctic regions and convergent over the oceanic regions just east of the Asian and North American continents. The condition reverses within the 280–290 K and 290–300 K layers (Figs. 4c and d) where strong mass divergence exists over oceanic regions while convergence occurs over the Arctic regions. Over the oceanic areas, strong sensible and latent heat release results in intense upward mass flux through isentropic surfaces (Fig. 3a). Downward mass flux through isentropic surfaces occurs over the Arctic regions in association with the net energy loss due to the excess of the sink of energy by infrared emission over other energy sources. The regions of the most intense upward mass flux associated with the strong heating in Fig. 3a lie over the cyclonic storm tracks of the northern Pacific and Atlantic Oceans. Through this mass circulation energy from the oceans is transported within the atmosphere to polar latitudes where radiative cooling prevails. As discussed earlier, the geostrophic mass advection within mid-latitude baroclinic disturbances is an integral part of the thermodynamically coupled mass circulations. The embedded direct cell over the higher latitudes of the Northern Hemisphere in the zonally averaged mass circulation (Fig. 2) is a reflection of this exchange (Townsend and Johnson, 1981).

This winter monsoonal flow beneath 300 K within polar and mid-latitudes also plays an important rôle in the maintenance of the distinct belt of polar westerlies (Fig. 1a). Note, the heating of polar air masses by mid-latitude oceanic sources of energy in Fig. 3 constitutes the upward diabatic mass flux near 35–50° N in the zonally averaged mass circulation (Fig. 2). Within Eliassen's (1951) perspective of the forcing of a vortex, westerlies result from mass circulations being forced by a combination of differential heating and torques (Gallimore and Johnson, 1981). The poleward geostrophic mode of mass transport that exists within the 290–300 K layer (Fig. 2) is linked with negative pressure torques that force poleward motion while below 280 K positive pressure torques force mass transport equatorward. As a consequence, absolute angular momentum is transported poleward within this thermodynamically forced mass circulation, and at the same time is also transferred from the upper to the lower branch of the mass circulation through the action of pressure stresses (Johnson and Downey, 1975a, b; Gallimore and Johnson, 1981). The sense of the cell implies an enhancement of the transport of absolute angular momentum from lower to higher latitudes as Townsend's (1980) results verify. This circulation is an integral part of the maintenance of the westerlies. If the oceanic sources of latent and sensible energies were absent in these regions, the distinct structure of the time-averaged polar jet stream would be absent or of a different character.

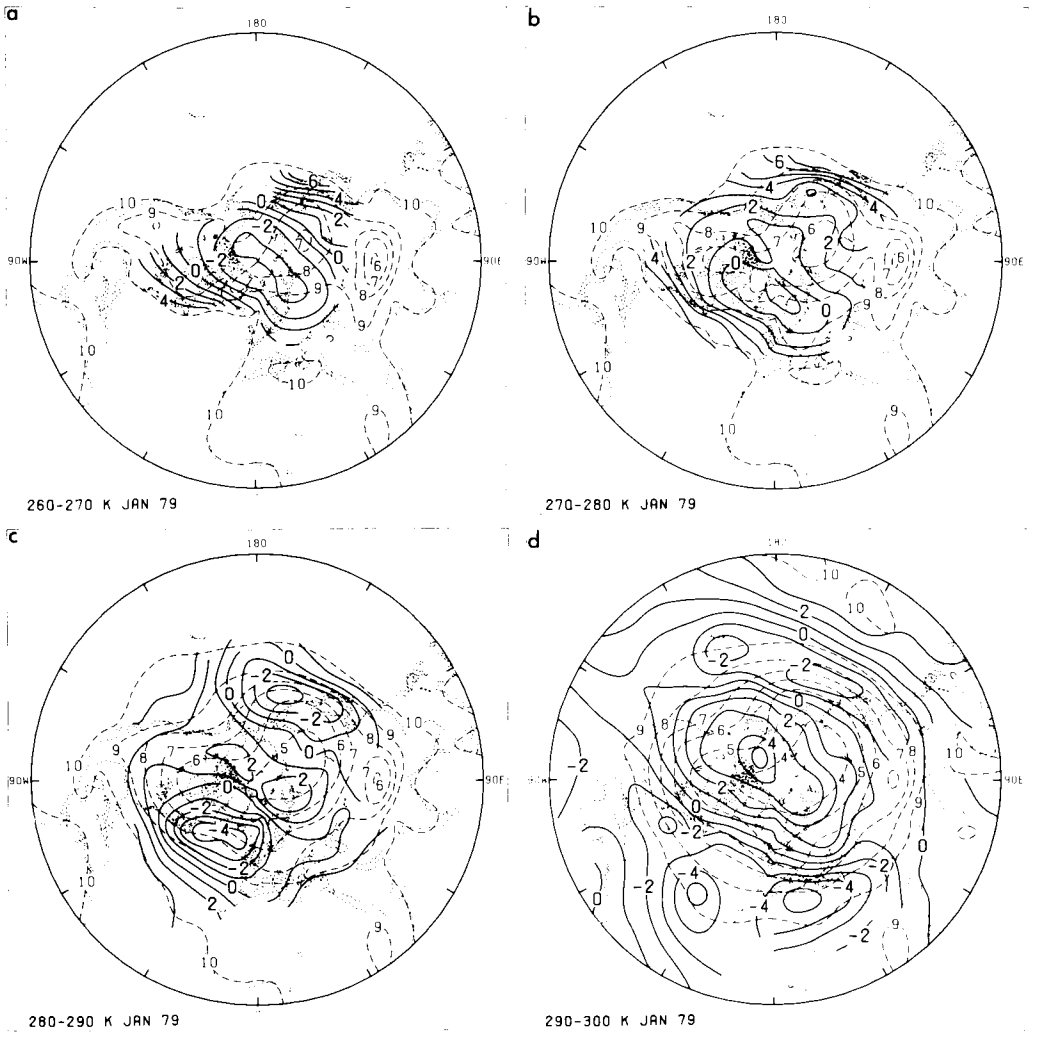

Fig. 4. Mass transport potential (solid contours) for 260–270 K (a), 270–280 K (b), 280–290 K (c) and 290–300 K (d) isentropic layers for the Northern Hemisphere of January 1979 (units, 10^8 kg K^{-1} s^{-1}). The potential field is contoured only where the isentropic layer is above the earth's surface. Legend same as Fig. 1.

4.2. The mean global transport of mass for April 1979

The irrotational and rotational modes of mass transport for April 1979 are presented in Fig. 5. In the rotational mode of mass transport (Figs. 5a and c) the circumpolar westerlies of both hemispheres in the 300–310 K and 340–350 K layers appear approximately equal in intensity except for the 300–310 K layer where the Southern Hemisphere westerly circulation is somewhat more intense. Well-developed anticyclonic circulations are found in the subtropics within the 300–310 K layer. The only anticyclonic circulation in the 340–350 K layer in April is located over the Philippines and to a large degree must be associated with the major tropospheric heat source over the western Pacific that is associated with convection; see Fig. 3b.

The seasonal movement of the primary heat source associated with the Asiatic monsoon from one hemisphere to the other is well illustrated in the

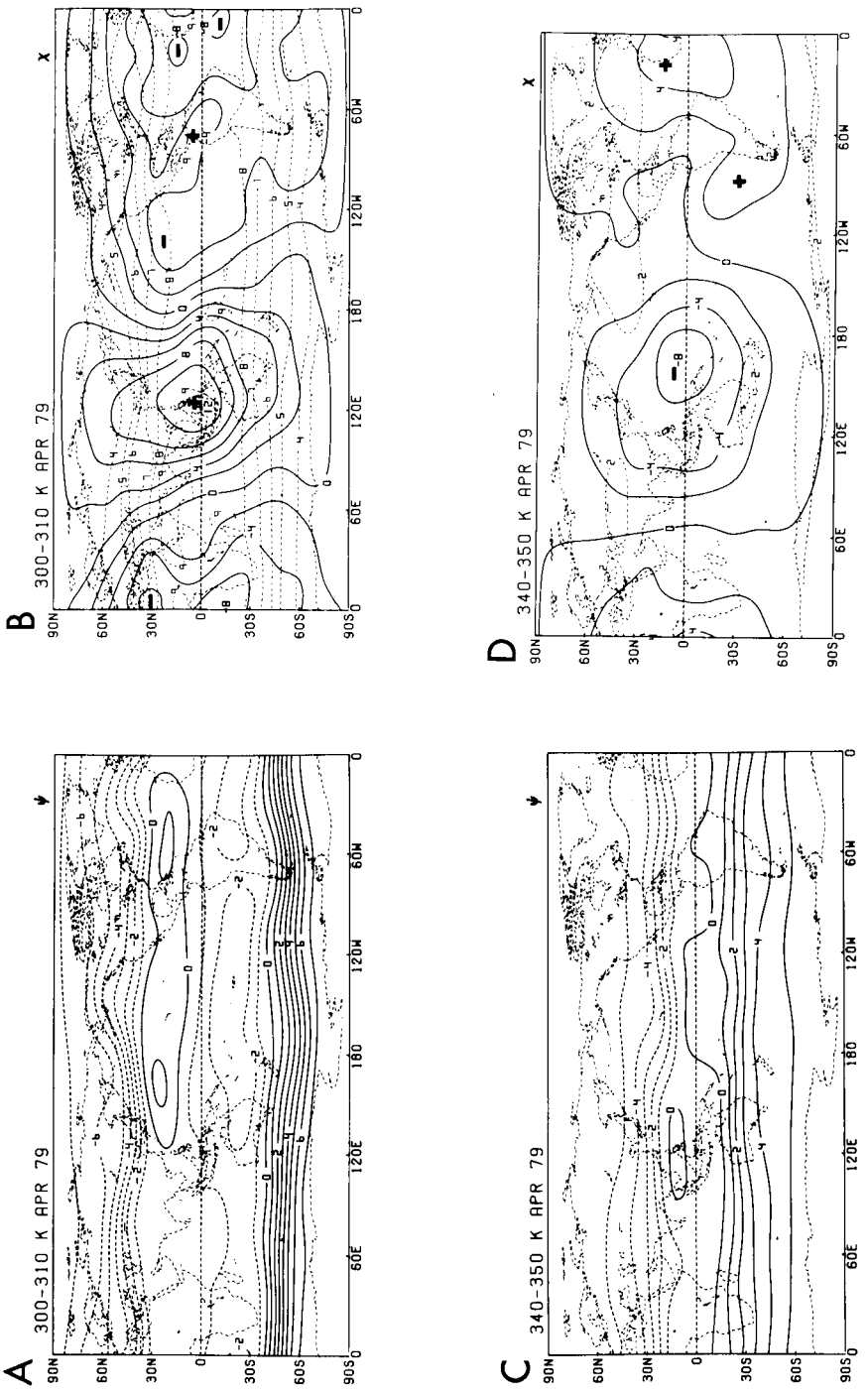

Fig. 5. Same as Fig. 1 except for April 1979.

potential functions of the four months selected for this study. In Figs. 5b and d the most prominent center of mass convergence within the 300–310 K layer and divergence within the 340–350 K layer lies over the equator north of New Guinea, which is northwest of its January location. The position of these centers coincides with the region of the maximum heating extending from the western Pacific to Indonesia in Fig. 3b. As in January, the general symmetry which exists in both north-south and east-west directions suggests that the Walker-type and Hadley-type circulations within the isentropic structure are of nearly equal importance in the transport of energy from source to sink regions.

Other centers of mass convergence and divergence are evident in tropical and subtropical latitudes. Note in Figs. 5b and d the paired nature of the maxima and minima of the potential function at the two levels over the western Pacific, eastern Pacific, Central and South America and the eastern Atlantic. Ascending branches of the mass circulation associated with heating over the ITCZ just north of the equator and the western Amazon basin in Fig. 3b are linked with descending branches associated with cooling over the eastern portions of the subtropical anticyclonic circulations in the Atlantic and Pacific oceans of both hemispheres. The longitudinal variation of the gradient in the potential function in higher latitudes suggests a great deal of zonal asymmetry of the meridional component of irrotational mass transport in polar latitudes. The irrotational components of mass transport across the poles in the 300–310 K layer is directed from the eastern Pacific–American–Atlantic sectors to the Asiatic–western Pacific sectors. Within the 340–350 K layer, the component is reversed. This feature must be linked to the dominance of the equatorial heat source in southern Asia, Indonesia, Philippines and western Pacific over its counterpart in the eastern Pacific-American Atlantic section (Fig. 3b).

4.3. The mean global transport of mass for July 1979

The mass transport potential and stream functions for the 300–310 K and 340–350 K isentropic surfaces, July 1979, are presented in Fig. 6. At the 300–310 K layer, the intense gradient of the mass stream function (Fig. 6a) is evidence of the strong westerlies of the Southern Hemisphere circumpolar vortex during its winter season. The pressure analysis shown in Fig. 6b again indicates the slope of this isentropic layer from below 800 mb in tropical latitudes to 300 mb over the Antarctic continent. The maximum slope in mid-latitudes of the Southern Hemisphere is evidence of the baroclinic support to the westerlies of the circumpolar vortex. Distinct anticyclonic circulations are indicated throughout the subtropics of the Southern Hemisphere. In the Northern Hemisphere, the Pacific and Atlantic subtropical anticyclones are also well developed. Note the clockwise circulation in the low troposphere of the Indian Ocean region as indicated by the rotational component of the mass circulation in 300–310 K layer. The easterly current at 15° S reaches from the eastern Indian Ocean to near Madagascar, and then crosses the equator and turns further to the northeast with clockwise curvature. Embedded within this flow is the Somali jet that transports heat and moisture for the maintenance of the convection in the Indian monsoon.

The westerlies in the high latitudes of the Northern Hemisphere, while weak, are most pronounced from the Pacific Ocean across northern Canada and the northern Atlantic. Over the Siberian portion of the Asiatic continent the gradient is extremely weak. The stream function in Fig. 6a indicates a weak cyclonic circulation over the high polar regions that is displaced towards the North American continent.

The mass stream function for the 340–350 K isentropic layer in July (Fig. 6c) shows a distinct anticyclonic circulation over the region from southeastern Asia to northern Africa that captures the mean position of the tropical easterly jet. Another anticyclonic circulation is located over the southern United States–Mexico region. A primary feature of the circumpolar vortex in this layer is the belt of the westerlies near 30° S of the Southern Hemisphere. The belt of westerlies is displaced equatorward from the westerlies within the 300–310 K layer and lies above the anticyclonic circulations of the lower troposphere. Similar to the January analysis in the Northern Hemisphere, this latitudinal displacement of the westerlies and the mid-latitude Hadley-type cell within the isentropic mass circulation (Townsend and Johnson, 1981, Fig. 2) suggests a distinction between westerlies at higher latitudes and the subtropical westerlies at lower latitudes. However, in this case, the embed-

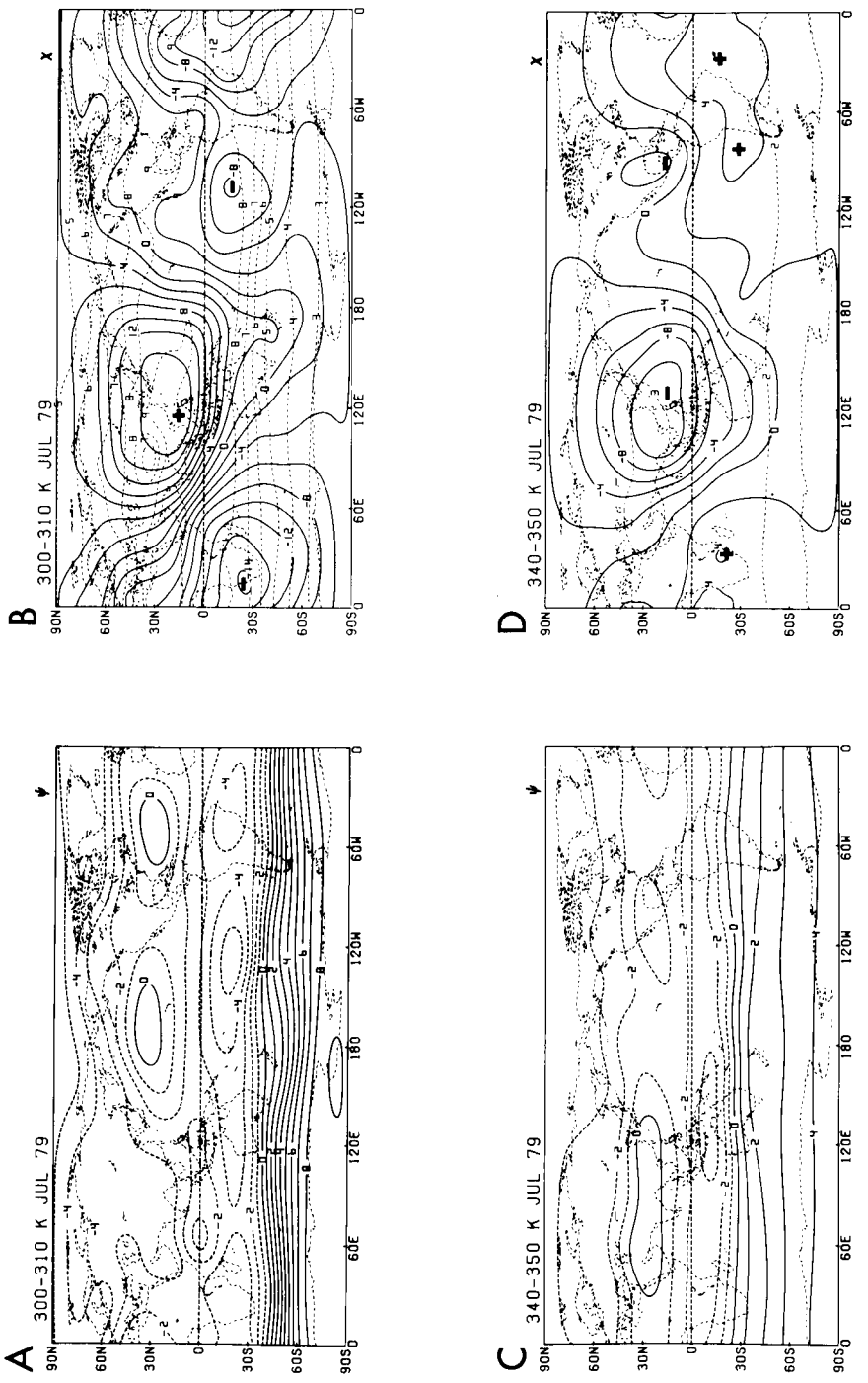

Fig. 6. Same as Fig. 1 except for July 1979.

ded mid-latitude Hadley-type cell of the Southern Hemisphere, as indicated in the July results of Townsend and Johnson (1981), is much weaker in comparison with its Northern Hemisphere winter counterpart and the latitudinal displacement is less pronounced. The comparison of the heating distributions in Figs. 3a and c suggests that diabatic heat sources in mid-latitudes of the Southern Hemisphere are less pronounced than their Northern Hemisphere counterpart, although it is possible that mass transport within the lower isentropic layers of the Southern Hemisphere was not resolved well in the NMC FGGE IIIa data set.

The mass transport potential for the 300–310 K (Fig. 6b) shows the dominance of the Asiatic monsoon. The intensity of irrotational mode of mass transport towards the broad maximum of the potential function over southeastern Asia and the South China Sea is strongest over the Indian Ocean and Arabian Sea. Intense irrotational mass transport towards the same center also occurs throughout Malaysia and the equatorial regions of the western Pacific. A secondary region of mass convergence is located over the Caribbean and Central America. These two regions coincide with relative maxima of heating in subtropical latitudes of the Northern Hemisphere (Fig. 3c). Within the subtropical latitudes of the Southern Hemisphere, centers of divergence of the mass transport in Fig. 6b which coincide with regions of diabatic cooling in Fig. 3c are located over the eastern portion of the Pacific and over the southern Atlantic-African region. The relative intensity and the scale of the irrotational mode show that isentropic mass circulations link these centers of divergence and net cooling with centers of convergence and net heating over southeastern Asia and the South China Sea.

At the 340–350 K isentropic level (Fig. 6d), the primary center of mass divergence over southeastern Asia is located above the lower tropospheric convergence within the 300–310 K layer. A secondary region of divergence occurs over the southwestern United States and Mexico. The regions of convergence in the southern Atlantic and eastern Pacific of the Southern Hemisphere lie over the regions of divergence within the 300–310 K layer.

It should be emphasized that these mass circulations primarily determine the sense of energy transport (Johnson et al., 1981). The latent energy release from convection in the region of the Asiatic monsoon is advected vertically to be exported to higher latitudes of both hemispheres and also longitudinally to the eastern Pacific and Atlantic sectors of the Southern Hemisphere. At the same time, the convergence of mass in the 300–310 K layer in the lower tropical troposphere over southeastern Asia provides a source of energy that helps to maintain the convection in these areas. Since this air, in part, lies within the planetary boundary layer in the tropical regions, the mass convergence is also linked with convergence of water vapor transport that supplies the latent energy during the excitation of convection. There is little doubt that the thermodynamically coupled mass circulation of the Asiatic summer monsoon plays a primary rôle in the entire planetary circulation through quasi-horizontal mass and energy transport.

Within the middle latitudes of the Southern Hemisphere, Fig. 3c shows pronounced regions of diabatic heating across the Pacific Ocean, south of Africa and southeastern Australia that are associated within baroclinic systems. At the same time, extensive regions of diabatic cooling are located eastsoutheastward of New Zealand and Africa which are associated with the prevalence of transient anticyclonic circulations in these regions (Hill, 1981).

4.4. The mean global transport of mass for October 1979

The irrotational and rotational modes of mass transport for October 1979 are presented in Fig. 7. In the rotational mode of mass transport (Figs. 7a, c), the circumpolar westerlies at the 340–350 K layer are approximately equal in both hemispheres, while at the 300–310 K layer, the Southern Hemisphere westerly mass transport is stronger. Subtropical anticyclonic circulation is well established within the 300–310 K layer. The only detectable anticyclonic circulation within the 340–350 K layer is located east-northeast of the Philippines and is associated with the deep tropical convection occurring in this portion of the Pacific. This convection is frequently associated with the occurrence of subtropical cyclonic circulations in the lower troposphere.

The pattern of the irrotational mode of mass transport in Fig. 7b again provides evidence of a planetary scale circulation linked with the tropical convection and heating in the western Pacific

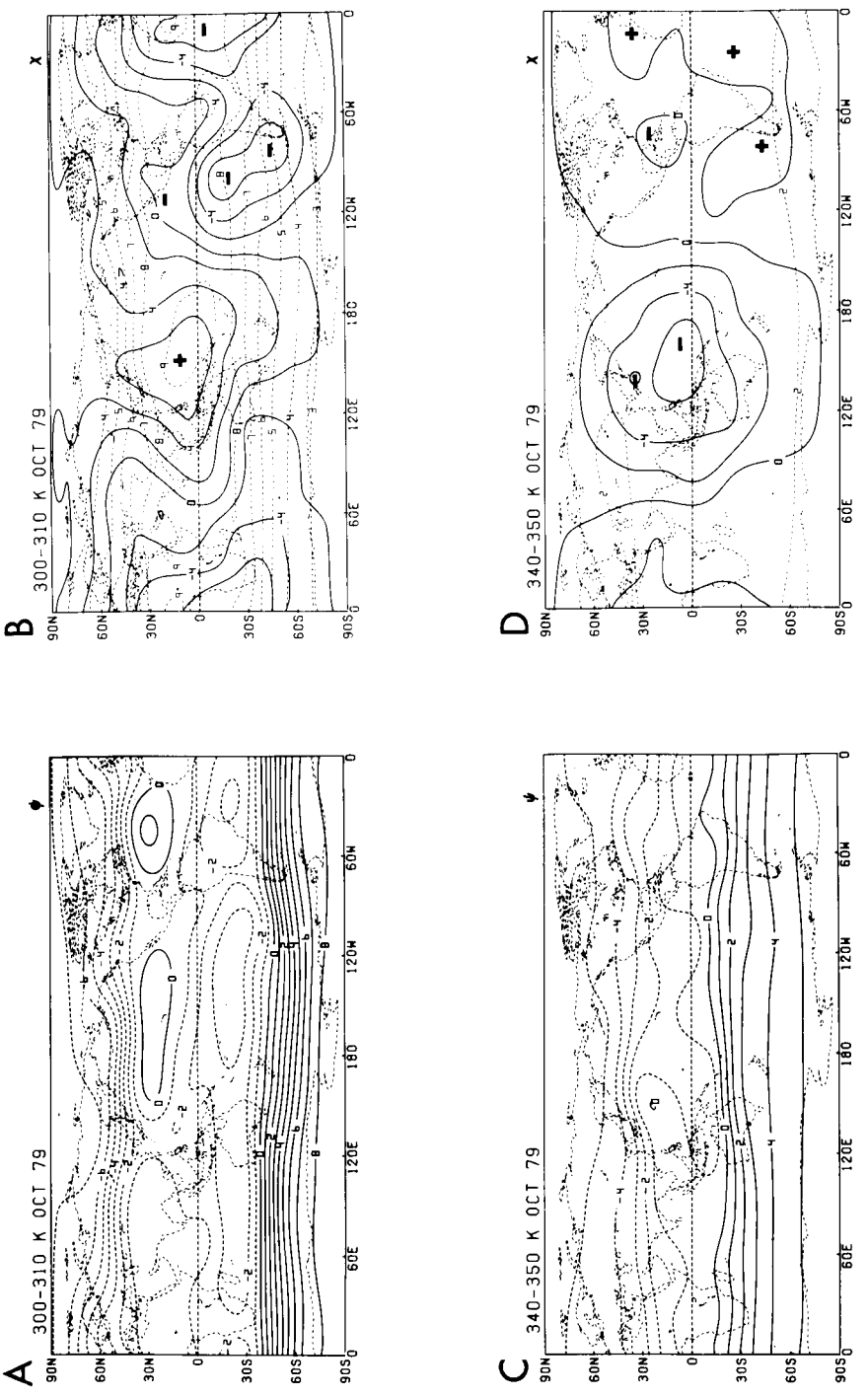

Fig. 7. Same as Fig. 1 except for October 1979.

shown in Fig. 3d. Note that the irrotational mass transport towards this center is largest to the southeast, the southwest and west. Through the tradewinds of the southern Pacific anticyclone, the irrotational mass transport from the southeast links this region with the eastern equatorial Pacific where downward vertical mass transport and net diabatic cooling prevails. The mass transport from the southwest is due to divergence within the Mascarene high. The other region of mass convergence within the 300–310 K isentropic layer is over Venezuela and the Caribbean. At the 340–350 K layer the pattern of the irrotational mode of mass transport is reversed.

The distribution of diabatic heating for October 1979 shown in Fig. 3d suggests that the intensity of differential heating at the planetary scale for October is less than the other three months; the patterns of relative extrema are less well defined with the exception of the cooling over the southern Pacific east of New Zealand. In the Northern Hemisphere, regions of heating along mid-latitude cyclonic storm tracks are being re-established as the winter season approaches.

5. Summary and conclusions

A preliminary analysis of the planetary scale mass transport and corresponding diabatic heating distributions determined from a FGGE Level IIIa data set generated by the National Meteorological Center have been presented. The transport was partitioned into rotational and irrotational components in order to isolate the thermodynamically coupled planetary scale circulations that link regions of heat sources and heat sinks. The results are presented in descriptive form in order to focus on an overview of global scale mass transport that was observed during FGGE and to examine the consistency of the NMC analyses generated by optimum interpolation. The descriptive discussion is also useful to gain familiarity with the nature of planetary scale mass exchange and its relation with differential heating within the isentropic framework.

Insight into the nature of planetary scale monsoonal exchange begins with the recognition that distinct physical mass circulations exist within the time-averaged flow that are uniquely coupled with differential heating. The time-averaged isentropic mass transport is determined by the time-averaged potential and stream functions. As such, the combination of the time-averaged potential and stream function fields determines the streamlines of time-averaged mass transport. Since the time-averaged potential and stream functions individually determine the vector fields $(\overline{\rho JU})_\chi$ and $(\overline{\rho JU})_\psi$, streamlines for the irrotational and rotational components of the time-averaged mass transport are separately and uniquely determined. Streamlines for the rotational motion remain independent of the diabatic mass flux in view of the non-divergent nature of this component. In contrast, the irrotational component of the motion and the flow streamlines defined by this component are directly related to vertical diabatic mass flux relative to isentropic surfaces. As such, the combination of the irrotational component of motion and diabatic mass flux uniquely determines a three dimensional structure for the thermodynamically coupled mass circulation in isentropic coordinates that is superimposed on the more intense rotational component of mass transport. Within this structure, however, streamlines should not be interpreted as trajectories of the time-averaged flow even though for a steady state field streamlines and trajectories would be coincident. The analyses are averages of non-steady circulation for which the streamlines of each event are not trajectories. Thus the streamlines of mass transport from time-averaged potential and stream functions cannot determine a time-average of Lagrangian trajectories.

The results for the rotational flow portray the circumpolar vortices of both hemispheres, subtropical anticyclones, the tropical easterly jet, and other features of the planetary scale circulation. The results for the irrotational component verify the global nature of monsoonal circulations which are linked to the planetary scale differential heating. The primary planetary source of energy in the region of Indonesia–Philippines–Southeast Asia is linked through quasi-horizontal mass transport with primary sink regions of energy in the two circumpolar vortices, the Sahara and subtropical anticyclonic circulations. This primary center of energy source moves seasonally from one hemisphere to the other. In January it is located southeast of New Guinea and northeast of Australia over the Pacific islands, by April it shifts due north to a position over the equator, by July it moves northwestward to the South China Sea and

by October it moves eastward to a position east of the Philippines and north of New Guinea. Sink regions of energy and corresponding centers of circulation also seasonally shift in position and vary in intensity. Other source regions of energy occur over Brazil in January and Central America and Africa in July.

Analysis also reveals a distinct thermodynamically coupled mass circulation in the polar and middle latitudes within the 260–300 K isentropic layers. The energy source regions associated with sensible and latent heating over mid-latitude oceanic regions east of the Asian and North American continents were linked by an irrotational mode of mass transport with the heat sink region over polar latitudes. The differential heating within these latitudes is responsible for the embedded Hadley-type cell of mid-latitudes in the isentropic zonally averaged mass circulation (Townsend and Johnson, 1981). The counterpart in the winter Southern Hemisphere is much weaker; this is most likely due to the lack of a mid-latitude heat source associated with the land-ocean contrast in the westerlies and the equatorward and eastward movement of extremely cold continental polar air masses over relatively warm oceans.

The relations between (1) the global distribution of boundary energy flux through the earth's surface and the top of the atmosphere, (2) heat sources and sinks internal to the atmosphere and (3) planetary scale mass and energy transport processes within the stratification of the atmosphere bear restating. Heating within a given region and cooling in another region result in net energy transport from the source to the sink region, a result basic to thermally forced circulations. The net energy transport is realized from the condition that more energy is transported by the horizontal branch in higher-valued isentropic layers from the heat source to the heat sink than is returned by the branch within lower-valued isentropic layers (Johnson et al., 1981). At the same time, no net mass exchange occurs. Thus a time-averaged isentropic mass circulation which is directly coupled to both mean energy transport and differential heating is manifested.

In the atmosphere, large-scale quasi-horizontal mass and energy transport between regions of heat sources and sinks tends to be adiabatic and inviscid. Since the statistical partition of transport processes within the isentropic structure provides for a mean mode of mass transport by both geostrophic and ageostrophic components of motion (Johnson and Downey, 1975a), the mode of mean transport of energy by the thermally coupled mean mass circulation can directly respond to satisfy energy balance requirements everywhere. This energy transport is mostly by ageostrophic mass circulations at low latitudes and partly by geostrophic motion at higher latitudes. Where the transition takes place, a handover in the component of transport from ageostrophic to geostrophic motion will occur that does not entail a change in the horizontal scale of transport within an isentropic layer. This degree of freedom allows the establishment of a direct link between the global scale of differential heating and the scale of response within the context of a temporally or zonally averaged mass circulation.

These features of isentropic analysis of planetary scale transport processes are important in establishing the relation between changes in thermodynamic forcing and the response of planetary scale circulations, particularly for longer time scales associated with seasonal, interannual and climatic variations. Within such time scales corresponding changes in differential heating and planetary scale exchange occur. The variations in intensity and/or position of circumpolar vortices, subtropical anticyclones and other large scale circulations are related with changes in the planetary scale monsoonal circulations that develop in direct response to the differential heating. It must be recognized that differential heating is determined through the combination of the external process of boundary energy flux and of the internal process of latent energy release within the resulting circulation. Since latent energy release primarily occurs within relatively small time and space scale mass circulations that are forced internally within the atmosphere through transient momentum exchange, the atmosphere's response to differential heating is neither separately determined by external boundary energy flux nor by internal dynamical mechanisms associated with transient momentum exchange.

6. Acknowledgments

We express our appreciation to Thomas Whittaker and Richard Selin for their computer pro-

gramming and data processing assistance, and to Nancy Malz, Jean Johnson and Gail Turluck for typing the manuscript. This research was jointly supported by the National Science Foundation and the National Oceanic and Atmospheric Administration under Grant nos. ATM 7822348 and ATM 8209757, and by the National Science Foundation under Grant Number ATM 8110678. The second author (Capt. Ronald D. Townsend) is pleased to acknowledge the research opportunity provided by the US Air Force Institute of Technology.

7. Appendix

List of symbols

U	Horizontal velocity
J	Jacobian for transformation of vertical coordinate to potential temperature $\lvert\partial z/\partial\theta\rvert$
p	Pressure, quasi-horizontal surface
θ	Potential temperature, quasi-horizontal surface
δ	Divergence of vector transport defined by (4)
ζ	Vertical component of curl of vector transport defined by (5)
χ	Transport potential function
ψ	Transport stream function
Subscripts	
χ	Designates irrotational component
ψ	Designates rotational component
p	Denotes isobaric coordinate system
θ	Denotes isentropic coordinate system
Operators	
$\bar{(\ )}$	Time average defined by $Y^{-1}\int_0^Y(\ )\,dt$
$\hat{(\ )}$	Mass-weighted time average defined by $\overline{\rho J(\ )}/\overline{\rho J}$
$\bar{(\ )}^{\theta}$	Vertical average defined by $(\theta_T-\theta_{s_0})^{-1}\int_{\theta_{s_0}}^{\theta_T}(\ )\,d\theta$
$\hat{(\ )}^{\theta}$	Mass-weighted vertical average defined by $\overline{\rho J(\ )}^{\theta}/\overline{\rho J}^{\theta}$
$\bar{(\ )}^{\theta,t}$	Vertically temporally averaged quantity $[Y(\theta_T-\theta_{s_0})]^{-1}\int_0^Y\int_{\theta_{s_0}}^{\theta_T}(\ )\,d\theta\,dt$
$\hat{(\ )}^{\theta,t}$	Mass-weighted vertically temporally averaged quantity
$\dot{(\ )}$	Substantial derivative with respect to time
$\partial/\partial t_{\theta(\text{or }p)}$	Local time derivative in isentropic (or isobaric) coordinates
$\nabla_{\theta(\text{or }p)}$	Quasi-horizontal Laplacian operator in tropic (or isobaric) coordinates
$\nabla^2_{\theta(\text{or }p)}$	Quasi-horizontal Laplacian operator in isentropic (or isobaric) coordinates

REFERENCES

Bengtsson, L., Kanamitsu, M., Kållberg, P. and Uppala, S. 1982. FGGE research activities at ECMWF. *Bull. Amer. Meteorol. Soc. 63*, 277–303.

Bergman, K. H. 1979. A multivariate optimum interpolation analysis system of temperature and wind fields. *Mon. Wea. Rev. 107*, 1423–1444.

Dutton, J. A. and Johnson, D. R. 1967. The theory of available potential energy and a variational approach to atmospheric energetics. *Adv. Geophys. 12*, 333–436.

Eliassen, A. 1951. Slow thermally or frictionally controlled meridional circulation in a circular vortex. *Astrophys. Norv. 5*, 19–60.

Fleming, R. J., Kaneskige, T. M. and McGovern, W. E. 1979a. The global weather experiment (I). The observational phase through the first special observing period. *Bull. Amer. Meteorol. Soc. 60*, 649–659.

Fleming, R. J., Kaneskige, T. M., McGovern, W. E. and Bryan, T. E. 1979b. The global weather experiment (II). The second special observing period. *Bull. Amer. Meteorol. Soc. 60*, 1316–1322.

Flohn, H. 1971. Tropical circulation pattern. *Bonner Meteorol. Abh. 15*, 55 pp.

Gallimore, R. G. and Johnson, D. R. 1981. The forcing of the meridional circulation of the isentropic zonally averaged circumpolar vortex. *J. Atmos. Sci. 38*, 583–599.

Hill, H. W. 1981. A synoptic case study using the FGGE buoy data of a typical low index regime in the western South Pacific Ocean. *ICSU/WMO GARP Conf. Proc. of Int. Conf. on Preliminary FGGE data analysis and results* (23–27 June 1980, Bergen, Norway), Geneva, 450–464.

Holloway, J. L. 1958. Smoothing and filtering of time series and space fields. *Adv. Geophys. 4*, 351–389.

Johnson, D. R. 1979. Systematic stratospheric-tropospheric exchange through quasi-horizontal transport processes within active baroclinic waves. *WMO Symp. on the long-range transport of pollutants and its relation to general circulation including stratospheric/tropospheric exchange processes*, October 1–5, 1979, Sofia, Bulgaria, WMO No. 538, 401–408.

Johnson, D. R. and Downey, W. K. 1975a. Azimuthally averaged transport equations for storms: Quasi-Lagrangian diagnostics (1). *Mon. Wea. Rev. 103*, 967–979.

Johnson, D. R. and Downey, W. K. 1975. The absolute angular momentum of storms: Quasi-Lagrangian diagnostics (2). *Mon. Wea. Rev. 103*, 1063–1076.

Johnson, D. R., Townsend, R. D., Wei, M. Y. and Selin, R. D. 1981. The global structure of energy transport within thermally-forced planetary scale mass circulation. *ICSU/WMO GARP Condensed Papers and Meeting Rep. of Int. Conf. on Early results of FGGE and large-scale aspects of its monsoon experiments* (12–17 January 1981, Tallahassee, Florida), Geneva, 1981, 3–27, 3–34.

Krishnamurti, T. N. 1961. The subtropical jet stream of winter. *J. Meteorol. 18*, 172–191.

Krishnamurti, T. N. 1971. Tropical east-west circulation during the northern summer. *J. Atmos. Sci. 28*, 1342–1347.

Krishnamurti, T. N., Kanamitsu, M., Koss, W. J. and Lee, J. D. 1973. Tropical east-west circulation during the northern winter. *J. Atmos. Sci. 30*, 780–787.

McPherson, R. D., Bergman, K. H., Kistler, R. E., Rasck, G. E. and Gordon, D. S. 1979. The NMC operational global data assimilation system. *Mon. Wea. Rev. 107*, 1445–1461.

Murakami, T. and Unninayar, M. S. 1977. Atmospheric circulation during December 1970 through February 1971. *Mon. Wea. Rev. 106*, 1024–1038.

NMC Staff Atmospheric Analysis Branch, 1979: Characteristics of FGGE Level IIIa data sets from the NMC global data assimilation system. *Preprint Vol., Fourth Conf. on Numerical weather prediction*, 29 October–1 November, 1979, Silver Spring, MD, 331–334.

Otto-Bliesner, B. L. and Johnson, D. R. 1982. Thermally-forced mean mass circulations in the Northern Hemisphere. *Mon. Wea. Rev. 110*, 916–932.

Shaw, Sir Napier, 1942. *Manual of meteorology, the physical processes of weather*, Vol. III. Cambridge University Press, 445 pp.

Townsend, R. D. 1980. A diagnostic study of the zonally-averaged global circulation in isentropic co-ordinates. Ph.D. thesis, University of Wisconsin, Madison, 221 pp.

Townsend, R. D. and Johnson, D. R. 1981. The mass and angular momentum balance of the zonally-averaged global circulation. *ICSU/WMO GARP Conf. Proc. of Int. Conf. on Preliminary FGGE data analysis and results* (23–27 June, 1980, Bergen, Norway), Geneva, 542–552.

Wei, M.-Y., Johnson, D. R and Townsend, R. D. 1983. Seasonal distributions of diabatic heating the First GARP global experiment. *Tellus 35A*, 241–255.

Young, D. 1962. The numerical solution of elliptic and parabolic differential equations. *Survey of numerical analysis*, J. Todd (ed.). McGraw-Hill, New York, 380–438.

Zillman, J. W. 1972. Isentropically time-averaged mass circulations in the Southern Hemisphere. Ph.D. thesis, University of Wisconsin, Madison, 205 pp.

Zillman, J. W. and Johnson, D. R. 1985. Thermally-forced mean mass circulations in the Southern Hemisphere. *Tellus 37A*, 56–76.